



International Conference
Nuclear Energy for New Europe 2004

Portorož • Slovenia • September 6-9

port2004@ijs.si
www.drustvo-js.si/port2004
+386 1 588 5247, fax +386 1 561 2276

PORT2004, Nuclear Society of Slovenia, Jamova 39, SI-1000 Ljubljana, Slovenia



Numerical Investigation of Natural Convection Heat Transfer in Volumetrically Heated Spherical Segments

Andrej Horvat

ANSYS Europe

Harwell International Business Centre

Fermi Avenue, Didcot, Oxfordshire, OX11 0QR

United Kingdom

andrej.horvat@ansys.com

Borut Mavko

Reactor Engineering Division

“Jožef Stefan” Institute

Jamova 39, SI-1000 Ljubljana, Slovenia

ABSTRACT

Numerical analysis of natural convection inside a heat generated fluid was performed for four different spherical geometries that match the experimental vessels used by Asfia et al. [5-7]. The transient calculations were performed with the CFX 5.7 fluid dynamic software. The simulations show that the highest heat flux is just below the rim of the cavity and it can be 50 times higher than at the bottom. Based on the numerical results, the local values of heat transfer coefficient and the distributions of global Nusselt number were calculated. The present, three-dimensional simulation results were compared with the numerical results of Mayinger et al. [3] and Reineke et al. [4], and with the experimental data of Asfia et al. [5-7]. The agreement between the results that is well inside the experimental scatter verifies the selected modeling approach.

1 INTRODUCTION

Natural convection in a volumetrically heated fluid is of significant importance in nature as well as in engineering applications. In the present work, our interest is focused on post-accident heat removal from accumulated molten core material in a reactor pressurized vessel (RPV) lower plenum. External cooling of a lower plenum by flooding the concrete cavity with subcooled water is one of the several management strategies for such case.

Extensive amount of experimental as well as numerical work has been done on this subject; a review can be found in [1-2]. Previous research [3-5] also indicated that natural convection is responsible for redistribution of heat in a melt pool and for high, unequally distributed thermal loads on the plenum walls. The objective of our work has been to set-up a computational model of natural convection flow due to internal heat generation in a spherical cavity, in order to verify the model against publicly available experimental data. For this purpose, we selected some of the experiments performed by Asfia and collaborators [5-7].

The cited authors used 4 different spherical bell jars with a diameter of 60.1, 43.65, 21.0 and 15.7 cm., respectively. The level of fluid inside a jar was also different for each case. The fluid was heated uniformly with a 750 W magnetron taken from a conventional microwave oven. For the working fluid, R-113 was chosen as it gave the most uniform heating rate. To provide an adequate cooling, the lower part of the jar was submerged into circulating water in a larger container. Although different cooling scenarios were tested, we have limited our analysis to isothermal wall conditions. It is important to note that it has been extremely difficult to exactly follow the experiments [5-7], as some of the crucial details were not reported.

The numerical analysis of the natural convection in a spherical cavity was performed with the CFX 5.7 fluid dynamic software. Based on the simulation results, local heat transfer coefficients and global Nusselt number distributions were obtained for Rayleigh numbers from $9 \cdot 10^{10}$ to $1.1 \cdot 10^{14}$. To verify the selected modeling approach, the calculated local heat transfer coefficient was compared with the experimental data of Asfia et al. [5-7]. In the comparison of the global Nusselt number distributions we also included the results of Mayinger et al. [3] and Reineke et al. [4].

2 MODELING APPROACH

2.1 Geometrical considerations and boundary conditions

Numerical analyses were performed for 4 different cases. In the first case, the spherical cavity had a radius of 30.8 cm and it was filled up to the top ($H/R = 1.0$) with the working fluid. In the remaining three cases, the spherical cavity had a radius of 21.83 cm, but the level of the working fluid in the cavity was different from case to case ($H/R = 1.0, 0.5$ and 0.23). The geometries used in all 4 simulation cases are presented in Fig. 1.



Figure 1: Geometries of the numerical simulation cases

In their work [5-7], Asfia and collaborators experimented with different cooling arrangements for the bell jar: open top, rigid top, rigid and cooled top, and the case with crust on the walls. From all these options, we used rigid, no-slip wall conditions on all boundaries. In all cases, we also assumed isothermal boundary conditions with constant wall temperature $T_{wall} = 25.4 \text{ }^\circ\text{C}$. This type of boundary conditions has been best documented in [5-7], as it has not required any additional information.

2.2 Material properties

The working fluid in our calculations was also R-113, which was considered at the selected pressure and temperature conditions (101325 Pa and 25.4°C) to be an incompressible liquid. In our model, the density of R-113 was approximated with a linear function

$$\rho = -2.323 \text{ kg m}^{-3} \text{K}^{-1} (T - 298.65 \text{ K}) + 1648.5 \text{ kg m}^{-3} \quad (1)$$

based on data found in [8]. All other material properties were constant: viscosity $\mu = 6.64 \cdot 10^{-4}$ kg m⁻¹s⁻¹, thermal conductivity $\lambda = 7.47 \cdot 10^{-2}$ W m⁻¹K⁻¹ and specific heat $c_p = 958$ J kg⁻¹ K⁻¹.

2.3 Turbulence modeling

The numerical simulations were performed for the range of Rayleigh numbers from $9 \cdot 10^{10}$ to $1.1 \cdot 10^{14}$, where the flow regime is turbulent. Therefore, an additional turbulence model was needed to approximate turbulent diffusion. We selected the shear stress transport (SST) model [9] as the appropriate choice. This model is a combination of the k - ω and the k - ϵ model:

$$\text{SST model} = F_1 \cdot (k\text{-}\omega \text{ model}) + (1 - F_1) \cdot (k\text{-}\epsilon \text{ model}), \quad (2)$$

where F_1 is a blending function that smoothly switches between the k - ω model in a wall proximity and the k - ϵ model far away from the wall. By switching between two models, the SST model has all characteristics of low-Reynolds number k - ϵ models with much larger robustness. Additionally, the original SST model was also extended to take into account turbulence production due to buoyancy in the fluid [10].

2.4 Numerical considerations

Three-dimensional numerical meshes generated to perform the analysis consisted of tetrahedrals and prisms, which were aligned with walls to better approximate the boundary layer. The mesh size was different from case to case (Table 1), but in all cases the average physical wall distance of the first layer of nodes (Y^+) was below 2.0.

Most time consuming part of natural convection simulation is achieving thermal equilibrium. Therefore, steady-state solid conduction simulations were performed first. After the steady-state was reached, the result files were used to initialize steady-state natural convection simulations. This cycle of steady-state thermal conduction and natural convection simulations was repeated a few times. When the thermal equilibrium was sufficiently close, the result files were used as initial conditions for transient natural convection simulations. The timesteps of these transient simulations are listed in Table 1. Their size was well below the Brunt-Vaisala frequency criterion.

Table 1: Overview of the settings for all simulation cases

Case	R [cm]	H/R	I_g [W/m ³]	Ra	No. nodes	Timestep [s]
1	30.8	1.0	4.41E+03	$1.11 \cdot 10^{14}$	337350	0.25
2	21.83	1.0	4.59E+03	$2.07 \cdot 10^{13}$	271653	0.25
3	21.83	0.5	1.10E+04	$1.55 \cdot 10^{12}$	174726	0.4
4	21.83	0.23	3.13E+04	$9.10 \cdot 10^{10}$	109267	0.5

3 RESULTS AND DISCUSSION

Due to internal heat generation, the fluid raises in the middle of the cavity. As it is cooled, it flows downward along the isothermal sidewall. Figures 2 and 3 show instantaneous velocity and temperature fields for cases 1 and 2, respectively.

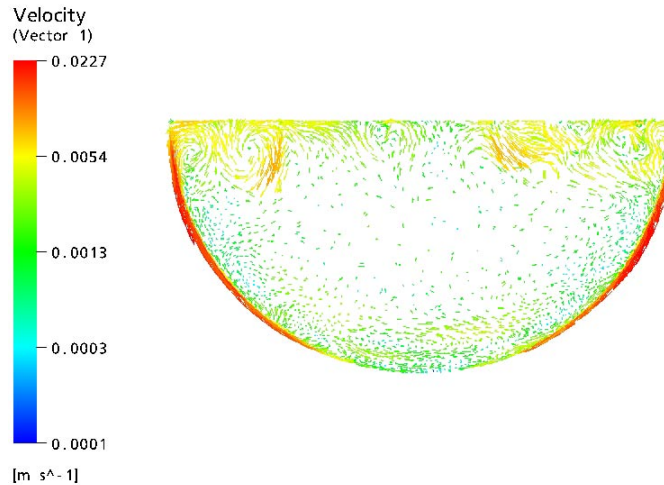


Figure 2: Velocity field in the cavity 1 (case 1)

In the lower part of the cavity, the fluid is thermally stratified and the flow field is almost steady. The upper part is under influence of large vortex structures that are triggered by Rayleigh-Taylor instabilities at the cooled top. As the Prandtl number is high in the considered cases ($Pr = 8.52$), the thermal boundary layer is much thinner than in the real core melt pool [2]. If the cooling from the top is increased, the flow pattern can become unstable and chaotic.

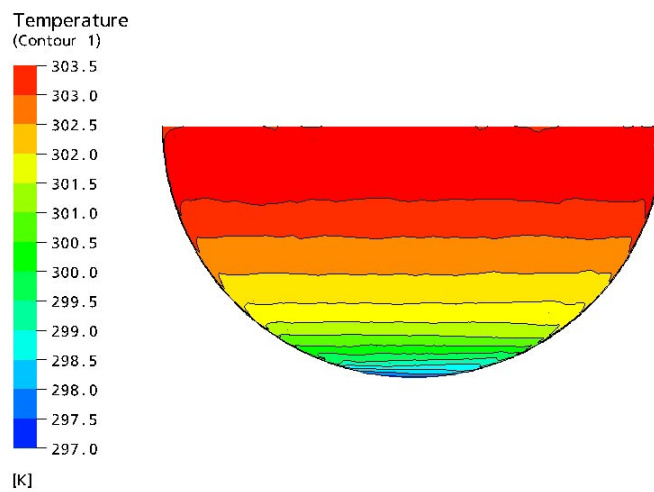


Figure 3: Temperature field in the cavity 2 (case 2)

Figure 4 shows the instantaneous heat flux on the wall of the cavity 1 (case 1). The situation is similar in all other cases. In general, heat flux is low at the bottom and increases with height. The highest heat flux is expected just below the rim of the cavity and it can be 50 times higher than at the bottom. This non-uniform heat flux distribution is the result of natural convection due to volumetric heat generation in the fluid. The changing form of flux contours also reveal time-dependent streaks of warm and cold fluid close to the wall.

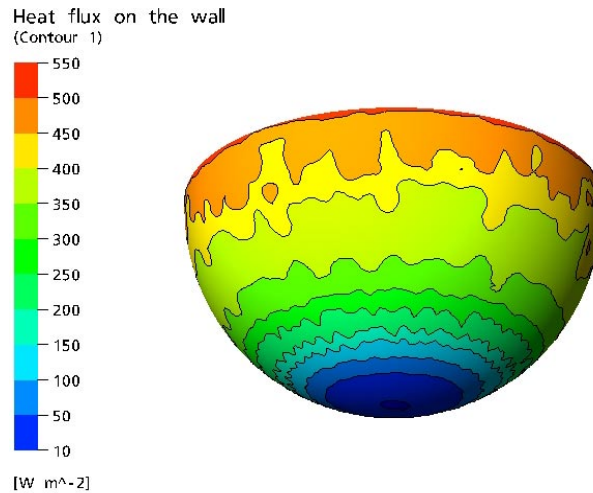


Figure 4: Heat flux on the wall of the cavity 1 (case 1)

The comparison with the experimental results of Asfia in collaborators [5-7] has been performed for the local wall heat transfer coefficient:

$$h = q_{wall} / (T_{wall} - T_{ave}), \quad (3)$$

which was averaged over the cavity perimeter and normalized with the wall average heat transfer coefficient. Two experimental runs were performed for this particular case (Fig. 5). The shape of the heat flux distribution on the cavity wall is parabolic. The calculated wall heat transfer coefficient matches the experimental values well inside the bounds of experimental scatter.

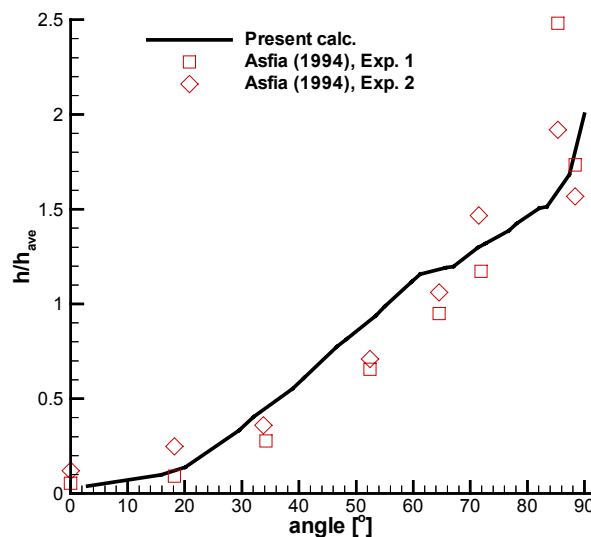


Figure 5: Comparison of wall heat transfer coefficients for the cavity 2 (case 2)

We have been trying to find a scaling law for the wall heat transfer coefficient h , which would connect all the cases. For this purpose, the local position is written as a local Rayleigh number:

$$Ra_{local} = \frac{c_p \rho^2 g \beta I_g V(z) z^2}{\lambda^2 \mu}, \quad (3)$$

where $V(z)$ is the volume of fluid at the level z . The heat transferred through the wall depends on the size of the wetted surface. Therefore, the local dimensionless heat transfer coefficient can be defined as

$$Nu_{local} = \frac{q_{wall} \alpha(z) R}{\lambda(T_{wall} - T_{ave})}, \quad (4)$$

where $\alpha(z)$ is the angle between the cavity wall and the vertical axis. Figure 6 shows the dependence of dimensionless variables Ra_{local} and Nu_{local} for all 4 cases. The similarity of the distributions is apparent and their values are close together. There are some discrepancies between cases 1 and 2, and cases 3 and 4, which arise from different importance of the top boundary on overall heat transfer. Namely, as the level of the fluid decreases (from $H/R = 1$ to $H/R = 0.5$ and 0.23), the total heat transfer on the top boundary increases on the account of the heat transfer through the sidewalls.

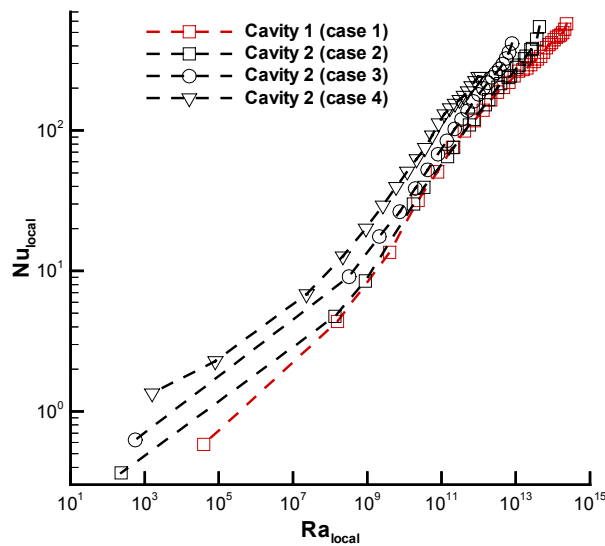


Figure 6: Local Nusselt number distribution.

The global Nusselt number distributions were compared with the correlation proposed by Mayinger et al. [3], who performed numerical calculations for a fully filled spherical cavity:

$$Nu = 0.55Ra^{0.2}. \quad (5)$$

Reineke et al. [4] also performed numerical analysis to determine global heat transfer coefficient on the wall of a partially filled spherical cavity with rigid cooled wall on the top. They obtained the following correlation:

$$Nu = 0.49Ra^{0.18}(H/R)^{0.29} \quad \text{for } H/R > 0.2. \quad (6)$$

Finally, the correlation derived by Asfia et al. [5-6] from the experimental measurements:

$$Nu = 0.54Ra^{0.18}(H/R)^{0.26}. \quad (7)$$

was also included in the comparison. Using the correlations (6) and (7) the Nusselt number distributions were calculated for both limiting cases i.e. $H/R = 1$ and 0.23 .

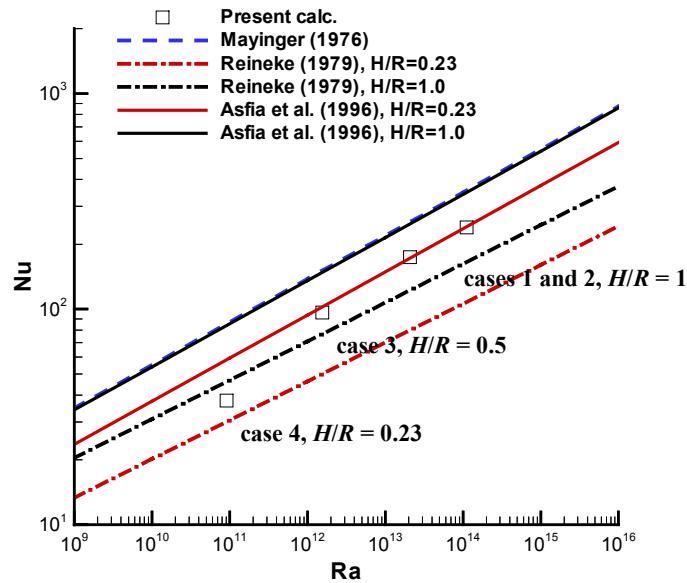


Figure 7: Comparison of global Nusselt number

Figure 7 presents the calculated global Nusselt number in comparison with the correlations (5-7). In general, our results agree well with the results of other authors. The calculated Nusselt numbers are no more than 5% apart from the correlation (6), and no more than 20% apart from the correlations (5) and (7).

4 CONCLUSIONS

In order to investigate cooling of core melt in a lower plenum during severe accident conditions, we built a numerical model of natural convection due to volumetric heat generation. Four different geometries were taken into consideration (Fig. 1). As our primary concern was the model verification, the geometries were selected from the experimental work of Asfia and collaborators, which is documented in the open literature [5-7].

The calculations were performed with the CFX 5.7 fluid dynamic software. The results of transient calculations reveal stable and thermally stratified lower part of the flow, and much more dynamic upper layer that is dominated by time dependent structures (Figs. 2-4). The heat flux is lowest at the stagnation point and increases along the spherical segment. The ratio of maximum and minimum heat transfer coefficient can be as high as 50.

Based on the simulation results, the distributions of local heat transfer coefficients along the wall were obtained and compared with the measurements of Asfia et al. [5-7]. The comparison shows good agreement with the experimental data. We also made a comparison of the calculated global Nusselt numbers with the correlations of Mayinger et al. [3], Reineke et al. [4], and Asfia et al. [5-7]. In general, our results are closer to the correlation defined by Reineke et al. [4]. Nevertheless, it should also be noted that the discrepancies with the correlations of other authors do not exceed 20%.

Overall, we are satisfied with the achieved agreement of the local heat transfer coefficients and the global Nusselt numbers, which in our opinion verifies the selected modeling approach and gives us confidence for future work.

NOMENCLATURE

c_p	specific heat	T	temperature
F_1	blending function in the SST model	T_{ave}	average temperature
g	gravity	T_{wall}	wall temperature
h	heat transfer coefficient	Y+	flow's physical wall distance
H	height of fluid in the vessel	Greek letters	
I_g	volumetric heat generation rate	α	angle between wall & vertical axis
k	turbulence kinetic energy	β	thermal expansivity
Nu	Nusselt number ($= q_{wall} H / \lambda (T_{wall} - T_{ave})$)	λ	thermal conductivity
Pr	$c_p \mu / \lambda$	ρ	density
q_{wall}	wall heat flux	ε	eddy dissipation
R	vessel radius	μ	dynamic viscosity
Ra	Rayleigh number ($= c_p \rho^2 g \beta I_g H^5 / \lambda^2 \mu$)	ω	turbulence eddy frequency

REFERENCES

- [1] R. R. Nourgaliev, T. N. Dinh, B. R. Sehgal, "Effect of Fluid Prandtl Number on Heat Transfer Characteristics in Internally Heated Liquid Pools with Rayleigh Numbers up to 10^{12} ", *Nucl. Eng. Design*, **169**, 1997, pp. 165-184.
- [2] A. Horvat, I. Kljenak, J. Marn, "Two-Dimensional Large Eddy Simulation of Natural Convection due to Internal Heat Generation", *Int. J. Heat Mass Transfer*, **44**, 2001, pp. 3985-3995.
- [3] F. Mayinger, M. Jahn, M. Reineke, V. Steinbrenner, Examination of Thermohydraulic Processes and Heat Transfer in a Core Melt, BMFT RS 48/1, Institut für Verfahrenstechnik der T.U., Hanover, Germany, 1976.
- [4] H. H. Reineke, Numerische Untersuchung der thermohydraulischen Vorgänge und des Wärmeüberganges in einer Karnschmelze bei kugelsegmentförmiger Geometrie und bei zufließendem Material von oben, BMFT RS 166-79-05, Band II A1, 1979.
- [5] F. J. Asfia, B. Frantz, V. K. Dhir, "Experimental Investigation of Natural Convection in Volumetrically Heated Spherical Segments", *J. Heat Transfer*, Trans. ASME, **118**, 1996, pp. 31-37.
- [6] F. J. Asfia, V. K. Dhir, "An Experimental Study of Natural Convection in a Volumetrically Heated Spherical Pool Bounded on Top with a Rigid Wall", *Nucl. Eng. Design*, **3**, 1996, vol. 163, pp. 333-348.
- [7] F. J. Asfia, Experimental Investigation of Natural Convection Heat Transfer in Volumetrically Heated Spherical Segments, Ph.D. Thesis, University of California, Los Angeles, 1995.
- [8] A. F. Mills, Heat and Mass Transfer, Irwin, 1995.
- [9] Z.R. Menter, "Zonal Two-Equation k-omega Turbulence Models for Aerodynamic Flows", *AIAA 93-2906*, 1993.
- [10] A. Horvat, Y. Sinai, Under-ventilated Compartment Fires (FIRENET), 2nd Progress Report, ANSYS Europe, June, 2004.